

# Drifting ~~Dynamics~~ dynamics of the Bluebottle (*Physalia physalis*)

Daniel Lee<sup>1,2</sup>, Amandine Schaeffer<sup>1,2</sup>, and Sjoerd Groeskamp<sup>3</sup>

<sup>1</sup>Coastal and Regional Oceanography Lab, School of Mathematics and Statistics, UNSW Australia, Sydney, New South Wales, Australia

<sup>2</sup>Centre for Marine Science and Innovation, UNSW Australia, Sydney, New South Wales, Australia

<sup>3</sup>NIOZ Royal Netherlands Institute for Sea Research, Texel, Netherlands

**Correspondence:** Daniel Lee (d.i.lee@unsw.edu.au)

**Abstract.** *Physalia physalis*, also called the Bluebottle in Australia, is a colonial animal resembling a jellyfish that is well known to beachgoers for the painful stings delivered by their tentacles. Despite being a common occurrence, the origin of the Bluebottle before reaching the coastline is not well understood, and neither is the way it drifts at the surface of the ocean. Previous studies used numerical models in combination with simple assumptions to calculate the drift of this species, excluding complex drifting dynamics. In this study, we provide a new parametrization for Lagrangian modelling of the Bluebottle by considering the similarities between the Bluebottle and a sailboat. This allows us to compute the hydrodynamic and aerodynamic forces acting on the Bluebottle and use an equilibrium condition to create a generalised model for calculating the drifting speed and course of the Bluebottle under any wind and ocean current conditions. The generalised model shows that the velocity of the Bluebottle is a linear combination of the ocean current velocity and the wind velocity scaled by a coefficient ('shape parameter') and multiplied by a rotation matrix. Adding assumptions to this generalised model allows us to retrieve models used in previous literature. We discuss the sensitivity of the model to different parameters (shape, angle of attack and sail camber) and explore different cases of wind and current conditions to provide new insights into the drifting dynamics of the Bluebottle.

## 1 Introduction

*Physalia physalis* (Fig. 1), also called the Indo-Pacific Portuguese man-of-war or the Bluebottle (*Physalia utriculus*, a synonym), is well known on the east coast of Australia for stinging tens of thousands of beachgoers each year (Surf Life Saving Australia: Sydney (2020)). The species is found throughout the world's oceans, in tropical, subtropical and (occasionally) temperate regions (Munro et al. (2019)). The Bluebottle resembles a jellyfish but is actually a siphonophore, a colonial organism composed of small individual animals called zooids (Totton and Mackie (1960)). There are four zooids depending on each other for survival and performing different functions, such as digestion (gastrozooids), reproduction (gonozooids) and hunting (dactylozooids). The last zooid, the ~~pnumatophore~~ pneumatophore, is a gas-filled float or sac that supports the other zooids and acts like a sail so the Bluebottle is constrained to the ocean surface, moving at the mercy of the wind, waves and marine currents. The Bluebottle's long tentacles hang below the float as they drift, fishing for prey to sting and drag up to their digestive zooids (Totton and Mackie (1960)).



**Figure 1.** Photograph of a Bluebottle taken at Coogee Beach, Sydney. Courtesy of Lisa Clarke.

25 For each Bluebottle, the float can be oriented towards the left or the right (dimorphism), believed to be an adaptation that prevents the entire population from being washed on shore to die (Totton and Mackie (1956), Woodcock (1944)). The "left-handed" Bluebottles sail to the right of the wind, while the "right-handed" Bluebottles sail to the left. The wind will always push the two types of Bluebottles in different directions, so at most half the population will be pushed towards the coast (Totton and Mackie (1956), Woodcock (1944)). The Atlantic Portuguese man-of-war (PMW) is considered the same species as the Bluebottle, but with key differences in their size and the number of long tentacles used for hunting. The Bluebottle's float rarely exceeds 10 cm and it has one long hunting tentacle that is less than 3 m in length (Fig. 1). In comparison, the PMW has

30

floats of up to 15 cm and several hunting tentacles that can reach 10 m in length 30 m in mature colonies when fully extended (Munro et al. (2019)).

Due to their inability to swim, the movement of the Bluebottle can be modelled by calculating the forces acting on it, or by  
35 advecting virtual particles in ocean and atmospheric circulation models. Previous studies modeled the movement of the PMW  
with Lagrangian particle tracking to explain major beaching events. For example, Ferrer and Pastor (2017) ~~where were~~ able  
to estimate the region of origin of a significant beaching event on the Basque coast in August 2010. They ran a Lagrangian  
model backwards in time, using wind velocity ( $V_A$ ) and a wind drag coefficient ( $\lambda = 4.5\%$ ) as drivers of the PMW motion  
( $V_{bb} = \lambda V_A$ ). They found that the region of origin was the North Atlantic Subtropical Gyre. Prieto et al. (2015) included both  
40 the effect of the surface currents ( $u$ ) and wind ( $V_{bb} = u + \lambda V_A$ ) to predict initial colony position of major beaching events in  
the Mediterranean in 2010. This model assumed the PMW was advected by the surface currents, with the effect of the wind  
being added with a much higher wind drag coefficient of 10%. Similarly, Headlam et al. (2020) used beaching and offshore  
observations to ~~run a similar hindcast~~ identify a region of origin, using the joint effects of surface currents and wind drag, for  
the largest mass PMW beaching on the Irish coastline in over 150 years.

These previous models made the key assumption that the PMW's sailing direction is the same as the wind direction. This  
45 may be based on the observation by Totton and Mackie (1960) that in winds stronger than force 4 (i.e. over 8 m/s 8 m s<sup>-1</sup>), the  
PMW would sail straight downwind with its sail parallel to the wind direction. However, it should be noted that this was a  
second-hand visual observation of one instance by a single individual. In addition, Totton and Mackie (1960) performed their  
own experiments and observed that in light winds (about 4 m s<sup>-1</sup>) the PMW balances itself at approximately 40°-40° to the  
50 wind (angle of attack), resulting in a completely different course of about 45° relative to the wind. In another experiment,  
Shannon and Chapman (1983) found that left- and right-handed specimens would separate by about 40° in force 7-8 winds  
(14-21 m s<sup>-1</sup>). This suggests a course of about 20° relative to the wind rather than both drifting downwind. More recently,  
Ferrer and González (2020) improved on the model from Ferrer and Pastor (2017) by analysing the same beaching event  
but incorporating dimorphism and different drift angles relative to the wind direction. They found different regions of origin  
55 depending on the drifting angle considered, and concluded that the PMWs were likely right-handed.

Iosilevskii and Weihs (2009) took a different approach by expressing the forces acting on the PMW. By considering the  
equilibrium condition of the aerodynamic (above water) and hydrodynamic (below water) forces, when the velocity of the  
PMW is constant, they derive equations that can be solved for the PMW's speed and direction of motion relative to the wind.  
However, they consider a situation with no background ocean current, where the hydrodynamic force is only the drag, opposed  
60 to the PMW course. Here we expand that model by adding the effect of the ocean current and simplifying the model down to  
an intuitive generalised vector form which could be implemented in Lagrangian models. We also analyze the impact of key  
variables such as angle of attack and sail camber (Sect. 4.3).

This paper is structured as follows. First we explain the methods and key assumptions used for our theoretical model (Sect. 2),  
followed by the force balance acting on the Bluebottle (Sect. 3). We then solve the equilibrium condition (Sect. 4.1), discuss  
65 the parameters in the model (Sect. 4.2 and 4.3) and apply the model to a few special cases that were chosen as instructive

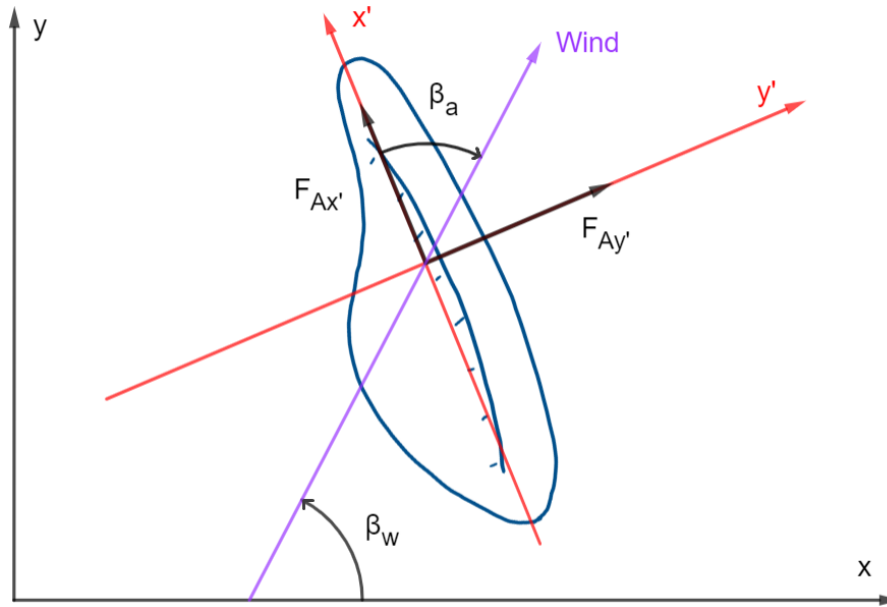


**Figure 2.** Top-down view of a left-handed (right-sailing) Bluebottle.  $x'$ ,  $y'$ ,  $x$  and  $y$  axes are defined above.  $F_{Ax'}$  and  $F_{Ay'}$  are the components of the aerodynamic force on the  $x'$  and  $y'$  axes respectively.  $\beta_a$  is the angle of attack.  $\beta_w$  is the angle of the wind.

examples of the Bluebottle's sailing dynamics (Sect. 5). Finally, we compare our results to previous studies and discuss some variables that were not included in the model (Sect. 6).

## 2 Methods

The Bluebottle undergoes similar forces as a sailboat. Therefore, like Iosilevskii and Weihs (2009), we consider the aerodynamic and hydrodynamic forces acting on the Bluebottle, as with a sailboat (Szelangiewicz and Żelazny, 2018). The aerodynamic force, generated by the wind blowing against the Bluebottle's sail (Fig. 2), is split into two components,  $F_{Ay'}$  (perpendicular to sail) and  $F_{Ax'}$  (parallel to sail), as shown in Fig. 2. The magnitude of the aerodynamic force is dependent on the wind speed, the area of the sail and the orientation of the Bluebottle to the wind, which we call the angle of attack  $\beta_a$  (Fig. 2). We also refer to the angle between the  $x$  axis and the wind as  $\beta_w$ , using the standard  $x$  and  $y$  axes, which are east/west and north/south respectively.

The hydrodynamic force is caused by the interactions of the water with the submerged body of the Bluebottle. The wind-driven motion of the Bluebottle through the water creates a hydrodynamic drag opposite to the direction of motion. The sum of the wind-driven drag and the bluebottle Bluebottle motion due to the background ocean current results in a relative current, which determines the total hydrodynamic force acting on the Bluebottle. Compared to Iosilevskii and Weihs (2009), we here add the effect of the ocean current but we do not consider the drag caused by the tentacles (see discussion in Sect. 6) and assume that the submerged part of the Bluebottle is a cylinder. This is a reasonable assumption since the Bluebottle has only

one tentacle which is much shorter than the PMW's tentacles. The submerged body is important for drag, but does not have a directional component to it because it is cylindrical. This differs from the submerged part of a sailboat, which has a long straight keel sticking down from the bottom of the boat. The keel minimizes sideways motion and rotation, allowing the boat to maximize forward motion. Since the Bluebottle's body has no keel and is assumed to be perfectly symmetrical, it does not restrict rotation and the orientation of the Bluebottle will be completely determined by the wind. Furthermore, the Bluebottle's motion will not be restricted by a keel, so it can move forward, sideways, or at any other angle with respect to its sail.

The forces acting on the Bluebottle will be expressed as components on two axes where the force coefficients and affected surface areas are most easily calculated. We call these the  $x'$  and  $y'$  axes and they are defined relative to the Bluebottle's sail. The  $x'$  axis is along the chord of the sail. The  $y'$  axis is perpendicular to the  $x'$  axis and goes through the centre of the sail, which is also assumed to be symmetric (Fig. 2). We use the axes labels as subscripts for variables that are related to specific axes. Any vectors in this paper are labelled in bold text and their components are the standard  $x$ - and  $y$ - components. Angles that are measured anticlockwise are considered positive, while angles that are measured clockwise are considered negative. The only exception to this is  $\beta$ , which is always considered positive starting from the  $x'$  axis (Fig. 3).

### 95 3 Forces acting on the Bluebottle

We now present the formulas that represent the aerodynamic and hydrodynamic forces acting on the Bluebottle. Compared to Iosilevskii and Weihs (2009), we choose not to consider the moment-force or the distances between the aerodynamic centre of effort and the hydrodynamic centre of effort, as these variables would require very rough estimates. Furthermore, Iosilevskii and Weihs (2009) do not use these variables in the final equations that describe the course and speed, but rather to analyze the PMW's sail contraction and tilting of their tentacles - which we don't consider here. The moment-force would result in a torque, and thus the orientation of the Bluebottle would be influenced by a combination of the wind and current conditions. However, similarly to the leeway methodology (discussed further in Sect. 6), the orientation behaviour of the Bluebottle (mainly represented by the angle of attack) can instead be determined by observations made in physical experiments.

#### 3.1 Aerodynamic force

105 The aerodynamic force on the Bluebottle  $F_A$  is expressed as components on the  $x'$  and  $y'$  axes. This can be represented by the standard aerodynamic force equation, often used for lift and drag force on an aeroplane wing for instance.

$$\begin{cases} F_{Ax'} &= \frac{1}{2}\rho_A S_{x'} V_A^2 C_{Ax'} \\ F_{Ay'} &= \frac{1}{2}\rho_A S_{y'} V_A^2 C_{Ay'} \end{cases} \quad (1)$$

where  $\rho_A$  is the density of the air (taken as  $1.225 \text{ kg m}^{-3}$ ),  $S_{x'}$  and  $S_{y'}$  are the areas of the sail in-perpendicular to the respective axis,  $C_{Ax'}$  and  $C_{Ay'}$  are the respective force coefficients, and  $V_A$  is the wind speed. Wind speed is used rather than relative wind speed because the speed of the Bluebottle is at least one order of magnitude smaller compared to the wind speed.

The areas  $S_{x'}$  and  $S_{y'}$  are fixed values for a particular Bluebottle. On the other hand, the force coefficients  $C_{Ax'}$  and  $C_{Ay'}$  are functions of the angle of attack  $\beta_a$ . Note that here we separately calculate the components of the aerodynamic force on two different axes. This is because the values of the  $x'$  and  $y'$  force coefficients and areas will vary significantly.

115 Considering the order of magnitude of the parameters ([discussed in section 4.2](#)), for wind speeds from 1 to 10  $\text{ms}^{-1}$ ,  $F_{Ax'}$  will range from  $7 \times 10^{-6}$  N to  $7 \times 10^{-4}$  N and  $F_{Ay'}$  will range from  $1 \times 10^{-4}$  N to  $1 \times 10^{-2}$  N.

### 3.2 Hydrodynamic force

The hydrodynamic force on the Bluebottle  $F_H$  is dependent on the relative current, which is the current felt by the Bluebottle as it is in motion. The magnitude of the hydrodynamic force can be represented by an equation of the same form as the aerodynamic force.

$$120 \quad F_H = \frac{1}{2} \rho_H S_H V_{RH}^2 C_H \quad (2)$$

where  $\rho_H$  is the density of the water (taken as  $1025 \text{ kg m}^{-3}$ ),  $S_H$  is the projected area of the submerged Bluebottle surface onto the Bluebottle's plane of symmetry,  $C_H$  is the force coefficient, and  $V_{RH}$  is the speed of the current relative to the Bluebottle (Fig. 3). Considering the order of magnitude of the parameters,  $F_H$  will range from  $1 \times 10^{-4}$  N to  $1 \times 10^{-2}$  N.

125 The hydrodynamic force  $F_H$  is calculated using a single equation, thus using just one value for both the area and the force coefficient. Unlike the aerodynamic force, we do not need to calculate two components of the force separately. This is because the submerged body of the Bluebottle is close to cylindrical, so there is not much variance in the value of the area or force coefficient. The relative speed of the current can be represented by

$$V_{RH} = \sqrt{V_{Hx}^2 + V_{Hy}^2} \quad (3)$$

[with](#)

$$130 \quad \begin{cases} V_{RHx} &= u - V_{bbx} \\ V_{RHy} &= v - V_{bby} \end{cases} \quad (4)$$

where  $V_{RHx}$  and  $V_{RHy}$  are the components of the relative velocity of the current in the respective axes,  $u$  and  $v$  are the x and y components of the ocean current velocity,  $V_{bbx}$  and  $V_{bby}$  are the x and y components of the Bluebottle velocity vector.

To later solve for the equilibrium condition (Sect. 4.1), when the velocity of the Bluebottle is constant, we require the hydrodynamic force on the  $x'$  and  $y'$  axes. This is represented by

$$135 \quad \begin{cases} F_{Hx'} &= F_H \cos \beta \\ F_{Hy'} &= F_H \sin \beta \end{cases} \quad (5)$$

where  $\beta$  is the angle between the  $x'$  axis and the relative velocity of the current (Fig. 3).

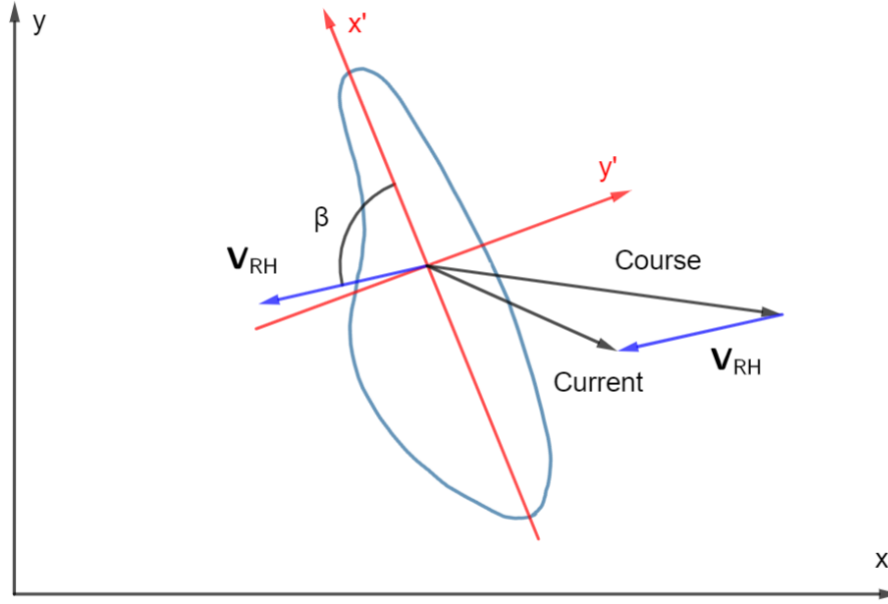


**Figure 3.** Relative current velocity  $V_{RH}$  is the difference between the ocean current velocity and the Bluebottle's velocity (called Course).  $\beta$  is the angle between the  $x'$  axis and the relative velocity of the current.

#### 4 Solving Bluebottle ~~Velocity~~ velocity

##### 4.1 Equations

We now solve for the equilibrium condition, where the velocity of the Bluebottle will be constant, hence there is no acceleration since the Bluebottle does not swim. Based on Newton's Second Law, this occurs when the net forces acting on the Bluebottle are zero. Hence, the aerodynamic and hydrodynamic forces must be equal in magnitude on each axis. Expressing the equilibrium conditions

$$\begin{cases} F_{Ax'} = F_{Hx'} \\ F_{Ay'} = F_{Hy'} \end{cases} \quad (6)$$

along the  $x'$  and  $y'$  axes yields the equations

$$\begin{cases} \rho_A S_{x'} V_A^2 C_{Ax'} = \rho_H S_H V_{RH}^2 C_H \cos \beta \\ \rho_A S_{y'} V_A^2 C_{Ay'} = \rho_H S_H V_{RH}^2 C_H \sin \beta. \end{cases} \quad (7)$$

Dividing the equations in (7) gives

$$\frac{S_{y'} C_{Ay'}}{S_{x'} C_{Ax'}} = \tan \beta \quad (8)$$

while taking the sum of squares of the equations in (7), then simplifying and taking the root gives

$$V_{RH}^2 = \frac{\rho_A V_A^2 \sqrt{(S_{x'} C_{Ax'})^2 + (S_{y'} C_{Ay'})^2}}{\rho_H S_H C_H}$$

$$150 \quad V_{RH} = \lambda V_A, \text{ where } \lambda = \sqrt{\frac{\rho_A \sqrt{(S_{x'} C_{Ax'})^2 + (S_{y'} C_{Ay'})^2}}{\rho_H S_H C_H}}. \quad (9)$$

~~We have found~~ This equation gives an expression for the coefficient  $\lambda$  (shape parameter), where previous studies have used constant values. We see that  $\lambda$  is based on the ratio of densities, Bluebottle areas and force coefficients. Note that  $\lambda$  is also dependent on the angle of attack  $\beta_a$ , since this affects the value of the force coefficients.

Once  $\beta$  and  $V_{RH}$  are known from Eq. (8) and Eq. (9), we calculate the velocity and course of the Bluebottle in terms of the  
 155 x and y axes. The x and y components of  $\mathbf{V}_{RH}$ , the relative velocity of the current, are

$$\begin{cases} V_{RHx} &= V_{RH} \cos \alpha \\ V_{RHy} &= V_{RH} \sin \alpha \end{cases} \quad (10)$$

where  $\alpha$  is the angle between the x axis and the relative current vector. Relating  $\alpha$  to known angles (Fig. 2) gives

$$\alpha = \beta - \beta_a + \beta_w, \text{ for a left-handed Bluebottle, for a left-handed Bluebottle (Fig. 8)} \quad (11)$$

$$\alpha = -\beta - \beta_a + \beta_w, \text{ for a right-handed Bluebottle, for a right-handed Bluebottle (Fig. A1)} \quad (12)$$

160 where  $\beta_w$  is the angle of the wind (between the x axis and the wind), and  $\beta_a$  is the angle of attack (between the  $x'$  axis and the wind, Fig. 2) and  $\beta$  is the angle between the  $x'$  axis and the relative velocity of the current (Fig. 3). Note that  $\beta$  is always considered positive. To find  $\alpha$  we choose a constant value for  $\beta_a$  (see Sect. 5 and Fig. 8). The absolute direction of the wind  
 $\beta_w$  should also be known.

Once  $\alpha$  is known, we find the velocity of the Bluebottle relative to the x and y axes using equations 4 and 10:-

$$165 \quad \begin{cases} V_{bbx} &= u - V_{RH} \cos \alpha \\ V_{bby} &= v - V_{RH} \sin \alpha. \end{cases} \quad (13)$$

Finally using equation-9: Eq. (9):

$$\begin{cases} V_{bbx} &= u - \lambda V_A \cos \alpha \\ V_{bby} &= v - \lambda V_A \sin \alpha. \end{cases} \quad (14)$$

Here we can see the Bluebottle velocity is a linear combination of the current velocity and wind velocity with some scaling and rotation. However, the velocity is non-linear with respect to the angle of attack, since both  $\alpha$  and  $\lambda$  are dependent on  $\beta_a$ .

170



This solution for the Bluebottle's velocity can be expressed in a generalised vector form. For a left-handed Bluebottle, we have

$$\begin{aligned}
\mathbf{V}_{\text{bb}} &= \mathbf{u} - \lambda V_A \begin{pmatrix} \cos \alpha \\ \sin \alpha \end{pmatrix}, \quad \text{with } \mathbf{u} = (u, v) \\
&= \mathbf{u} - \lambda V_A \begin{pmatrix} \cos(\beta - \beta_a + \beta_w) \\ \sin(\beta - \beta_a + \beta_w) \end{pmatrix} \\
175 \quad &= \mathbf{u} - \lambda V_A \begin{pmatrix} \cos(\beta - \beta_a) \cos \beta_w - \sin(\beta - \beta_a) \sin \beta_w \\ \sin(\beta - \beta_a) \cos \beta_w + \cos(\beta - \beta_a) \sin \beta_w \end{pmatrix}.
\end{aligned}$$

Now using the x and y components of the wind velocity,  $V_{Ax} = V_A \cos \beta_w$  and  $V_{Ay} = V_A \sin \beta_w$ , we have

$$\begin{aligned}
\mathbf{V}_{\text{bb}} &= \mathbf{u} - \lambda V_{Ax} \begin{pmatrix} \cos(\beta - \beta_a) \\ \sin(\beta - \beta_a) \end{pmatrix} - \lambda V_{Ay} \begin{pmatrix} -\sin(\beta - \beta_a) \\ \cos(\beta - \beta_a) \end{pmatrix} \\
&= \mathbf{u} - \lambda \begin{pmatrix} \cos(\beta - \beta_a) & -\sin(\beta - \beta_a) \\ \sin(\beta - \beta_a) & \cos(\beta - \beta_a) \end{pmatrix} \begin{pmatrix} V_{Ax} \\ V_{Ay} \end{pmatrix} \\
&= \mathbf{u} - \lambda \begin{pmatrix} \cos(\beta - \beta_a) & -\sin(\beta - \beta_a) \\ \sin(\beta - \beta_a) & \cos(\beta - \beta_a) \end{pmatrix} \mathbf{V}_A.
\end{aligned}$$

180 Using the trigonometric identities  $\cos \theta = -\cos(180^\circ - \theta)$  and  $\sin \theta = \sin(180^\circ - \theta)$  we have

$$\mathbf{V}_{\text{bb}} = \mathbf{u} + \lambda \begin{pmatrix} \cos(180^\circ - \beta + \beta_a) & \sin(180^\circ - \beta + \beta_a) \\ -\sin(180^\circ - \beta + \beta_a) & \cos(180^\circ - \beta + \beta_a) \end{pmatrix} \mathbf{V}_A$$

~~And~~ and finally:

$$\mathbf{V}_{\text{bb}} = \mathbf{u} + \lambda \mathbf{R}(180^\circ - \beta + \beta_a) \mathbf{V}_A \tag{15}$$

where  $\mathbf{R}$  represents the rotation matrix. Similarly, for a right-handed Bluebottle we have

$$185 \quad \mathbf{V}_{\text{bb}} = \mathbf{u} + \lambda \mathbf{R}(180^\circ + \beta + \beta_a) \mathbf{V}_A. \tag{16}$$

These results show that the velocity of the Bluebottle is a linear combination of the ocean current velocity vector  $\mathbf{u}$  and the wind velocity vector scaled by the shape parameter  $\lambda$  and multiplied by a clockwise rotation matrix of  $180^\circ - \beta + \beta_a$ . This can be interpreted as the Bluebottle simply drifting with the current, while the force imparted by the wind on the sail is a proportion ( $\lambda$ ) of the wind velocity at an angle of  $180^\circ - \beta + \beta_a$  clockwise from the wind direction.

190 We refer to equations 15 and 16 as a generalised vector form. By adding assumptions, we can simplify our form to match Lagrangian models seen in previous literature. Hence we can explain the assumptions required to use these previous models. This vector form is the link between the practical papers that used simple vector models (Ferrer and Pastor (2017), Ferrer and González (2020), Prieto et al. (2015)) and the theoretical bottom-up approach used by Iosilevskii and Weihs (2009).

## 4.2 Determining ~~Parameters~~parameters

195 The formulation shown in equations 15 and 16 for the velocity of the Bluebottle depends on several parameters. Firstly, we will consider the parameters required to find the shape parameter  $\lambda$  (see ~~equation-9~~Eq. (9)).

The areas required were measured from photographs taken at Coogee beach, Sydney on 23/01/2019.  $S_{y'}$  (area of the Bluebottle's sail on the  $y'$  axis) was measured by estimating the area as a segment of a circle. This gave a value of  $3\pi - \frac{9\sqrt{3}}{4} \text{ cm}^2$  (approx  $5.5 \text{ cm}^2$ ).  $S_{x'}$  (area of the Bluebottle's sail on the  $x'$  axis) was measured by estimating the area as a triangle. This gave  
200 a value of  $1.12 \text{ cm}^2$ .

~~The force coefficients  $C_{Ax'}$  and  $C_{Ay'}$  depend on the orientation of the Bluebottle relative to the wind, which is measured by the angle of attack  $\beta_a$ .  $C_{Ax'}$  does not need to be estimated accurately because its value has little effect on the Bluebottle's course and speed, since the product  $S_{x'}C_{Ax'}$  (used in equations 8 and 9) is  $O(10^{-5})$  while  $S_{y'}C_{Ay'}$  is  $O(10^{-4})$ . Hence for  $C_{Ax'}$  we use the same constant value as Iosilevskii and Weihs (2009) of 0.1.  $C_{Ay'}$  is calculated using an expression derived by  
205 Iosilevskii and Weihs (2009) which estimates  $C_{Ay'}$  as a function of angle of attack (Sect. ??). Sect. 5 presents examples with different angles of attack and the resulting effect on the Bluebottle's course and speed.~~

We assume the submerged body of the Bluebottle is a cylinder, so  $S_H$  will be the rectangular cross section made by cutting through the cylinder's diameter. This is measured as  $3.78 \text{ cm}^2$ . Note the tentacles are not taken into account since they can retract or vary their angle.  $C_H$  can be estimated as the drag coefficient of a cylinder, which is dependent on Reynolds number.  
210 Reynolds number (for sea water) is defined as

$$\text{Re} = \frac{\rho_H u L}{\mu} \quad (17)$$

where  $u$  is the current speed with respect to the Bluebottle (order  $0.1\text{-}1 \text{ m s}^{-1}$ ),  $L$  is the characteristic length dimension (simply the diameter for a cylinder, which is  $0.027 \text{ m}$ ), and  $\mu$  is the dynamic viscosity of sea water (order  $10^{-3} \text{ Pa s}$ , dependent on temperature). This gives a Reynolds number between 2781 and 27810 (turbulent flow). For these values, the drag coefficient  
215 of a cylinder is very close to 1, so we estimate  $C_H$  as 1.

## 4.3 Influence of angle of attack: force coefficient

~~Iosilevskii and Weihs (2009) The force coefficients  $C_{Ax'}$  and  $C_{Ay'}$  depend on the orientation of the Bluebottle relative to the wind, which is measured by the angle of attack  $\beta_a$ .  $C_{Ax'}$  does not need to be estimated accurately because its value has little effect on the Bluebottle's course and speed, since the product  $S_{x'}C_{Ax'}$  (used in equations 8 and 9) is  $O(10^{-5})$  while  $S_{y'}C_{Ay'}$   
220 is  $O(10^{-4})$ . Hence for  $C_{Ax'}$  we use the same constant value as Iosilevskii and Weihs (2009) of 0.1.~~

Iosilevskii and Weihs (2009) derive the following expression for the force coefficient  $C_{Ay'}$  as a function of angle of attack by considering the aerodynamic forces acting on a wing surface (slender sail theory).

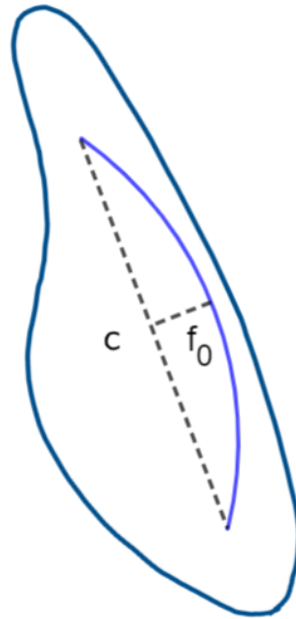


**Figure 4.** Camber of a BB-Bluebottle sail.  $f_0$  is the sail camber and  $c$  is the sail chord.

$$\begin{aligned} C_{Ay'} &= \frac{\pi A}{2} \beta_a + \frac{4\pi A}{3} \frac{f_0}{c} \\ \underline{A} &= \underline{\frac{b^2}{S_{y'}}} \end{aligned}$$

225

$$\begin{aligned} C_{Ay'} &= \frac{\pi A}{2} \beta_a + \frac{4\pi A}{3} \frac{f_0}{c} \\ \underline{A} &= \underline{\frac{b^2}{S_{y'}}} \end{aligned} \tag{18}$$

where  $A$  is the aspect ratio of the sail (calculated using  $b$ , the sail height, and  $S_{y'}$ , the sail area),  $\beta_a$  is the angle of attack (see Fig. 2),  $f_0$  is the sail camber and  $c$  is the sail chord (Fig. 4).  $f_0/c$  is referred to as the camber ratio.

230 Using our Bluebottle measurements, we have an aspect ratio of roughly 0.35 (half the value used by Iosilevskii and Weihs (2009), whose estimates were based on the PMW) and a sail chord of 5.2cm.

~~However, there are two concerns with using this expression. Firstly, It should be noted that in aerodynamic theory (for example Abbott et al. (1945)), it has been found that the lift coefficient of an airfoil increases roughly linearly with angle of attack until the lift coefficient approaches a maximum. This ~~behaviour is not considered in this expression.~~~~

235 Secondly, Totton and Mackie (1960) reported that in winds stronger than force 4 (i.e. over 8m/s), the PMW would sail  
straight downwind with its sail parallel to the wind direction (angle of attack of zero). Our model results do expression  
does not take this observation into account if we use the above expression for  $C_{Ay'}$  with 1% camber (the camber value  
used by Iosilevskii and Weihs (2009)). Instead of a course straight downwind for strong winds, we calculate a Bluebottle  
240 course of about  $36^\circ$  from the wind. This discrepancy could be solved by ignoring the observation, since it was a second-hand  
visual observation by a single individual. However, another explanation is perhaps that the camber ratio is far smaller than  
Iosilevskii and Weihs (2009) estimated. This is possible since their estimate of 1% was arbitrary. maximum into account.  
Despite these concerns, for now this expression remains to be our best method for estimating the value of the force coefficient  
 $C_{Ay'}$  and will be used throughout this study.

### 4.3 Influence of angle of attack ~~:-overall~~ on Bluebottle course

245 In this section we discuss two key parameters: the angle of attack and the sail camber. These are related to the aerodynamic  
force, so we will assume there is no current and examine how changing the angle of attack varies the Bluebottle's course relative  
to the wind. Firstly, a change in the angle of attack means the orientation of the Bluebottle relative to the wind is changing.  
This results in a different course relative to the wind. Secondly, the force coefficient  $C_{Ay'}$  changes based on the angle of attack,  
which then also varies the Bluebottle's course (Equation 8) Eq. (8).

250 Furthermore From the parametrization of  $C_{Ay'}$  (Eq. (18)), the effect of the angle of attack on the Bluebottle's course is  
dependent on the camber of the sail (Fig. 5). However, Fig. 5 shows. Figure 5 illustrates such a link, showing that the camber  
is only relevant at low angles of attack ( $0^\circ$  to  $10^\circ$ ). At higher angles of attack the relationship between angle of attack and  
the Bluebottle course relative to the wind becomes linear. This is because  $C_{Ay'}$  has become sufficiently large and hence the  
change in  $C_{Ay'}$  is insignificant. At this point, a  $10^\circ$  change in the Bluebottle's orientation simply results in a  $10^\circ$  change in  
255 the Bluebottle's course. As the camber becomes large,  $C_{Ay'}$  becomes sufficiently large even at zero angle of attack, and the  
relationship tends towards linearity.

At an angle of attack of zero, the Bluebottle is drifting. Previous modelling studies assumed a course straight downwind,  
which corresponds to a Bluebottle course of zero relative to the wind. This behaviour has been described by Totton and Mackie (1960)  
, who reported that in winds stronger than force 4 (i.e. over 8 m s<sup>-1</sup>), the PMW would sail straight downwind with its sail par-  
260 allel to the wind direction and a slight change in camber will determine the course (Fig. 6). If there is 6a). This corresponds to  
an angle of attack of zero but, according to our model, this behaviour would only occur if the Bluebottle sail has 0% camber  
(Fig. 5). In this case, the wind will only hit the side of the Bluebottle's sail and the Bluebottle's course will also be parallel  
to the wind direction. However, if there is camber, the Bluebottle will be pushed sideways (perpendicular to sail) even at zero  
angle of attack -(Fig. 6b). Due to this, as the camber increases, the course tends towards being perpendicular with to the wind  
265 at zero angle of attack -(Fig. 5).

At The Bluebottle course straight downwind can also be explained by an angle of attack of  $90^\circ$  (Fig. 5). At this angle of  
attack the Bluebottle's sail is perpendicular to the wind direction. We see that, at any camber the Bluebottle's course is parallel

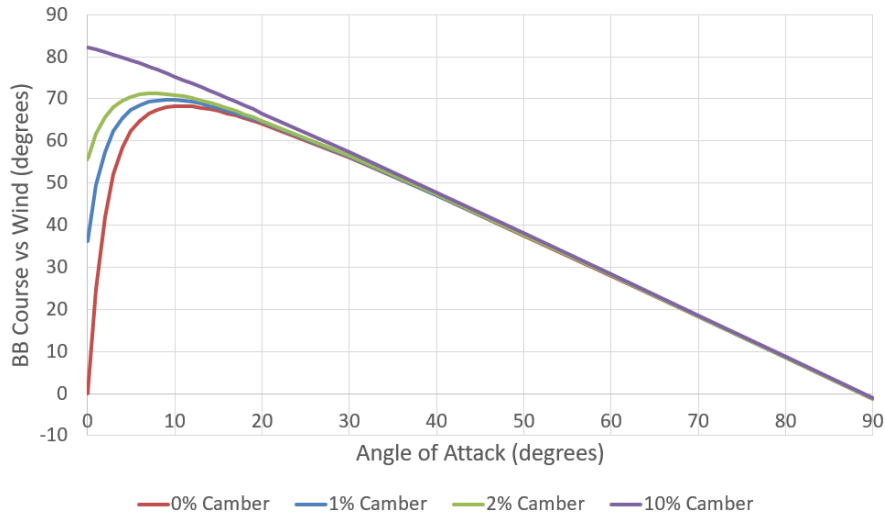


**Figure 5.** Bluebottle course relative to the wind ~~vs~~ (0 degree means a downwind course) as a function of angle of attack (0 degree means sail parallel to the wind) for different sail camber ratios.

to the wind direction and perpendicular to its sail (Fig. ??). However, to our knowledge, this situation has not been reported from observations, and it seems unlikely that the Bluebottle balances itself perpendicular to the wind.

270 At an angle of attack of  $90^\circ$ , the Bluebottle will sail downwind with sail perpendicular to the wind direction. This occurs at any camber. However, this Bluebottle orientation has not been observed.

## 5 Special Cases

### 5.1 Model and Assumptions for Downwind Drift

We now discuss the assumptions required to reduce our generalised vector form to simpler models seen in some previous studies. Firstly, we must assume the Bluebottle drifts straight downwind with its sail parallel to the wind direction under all conditions; despite the observation by Totton and Mackie (1960) that the PMW sails in this manner only in winds stronger than force 4 (i.e. over  $8\text{m/s}$ ). Considering a downwind drift, the sail orientation corresponds to an angle of attack  $\beta_a$  of  $0^\circ$  (Fig. 6). Substituting this into our vector form (Equation 15) gives Eq. (15) gives

$$\mathbf{V}_{\text{bb}} = \mathbf{u} + \lambda \mathbf{R}(180^\circ - \beta) \mathbf{V}_A.$$

280 Now, the Bluebottle will only sail straight downwind if the force coefficient  $C_{A_{y'}}$  equals zero, resulting in no aerodynamic force perpendicular to the sail (Fig. 7). At an angle of attack of zero, we expect  $C_{A_{y'}}$  to equal zero only if there is no camber (Fig. 5). Hence we must also make this assumption that the sail camber is zero. Based on equation 8 Eq. (8) and the fact that the relative current will always be opposite the wind (in order to have an equilibrium condition), we have  $\beta = 180^\circ$  (Fig. 7),

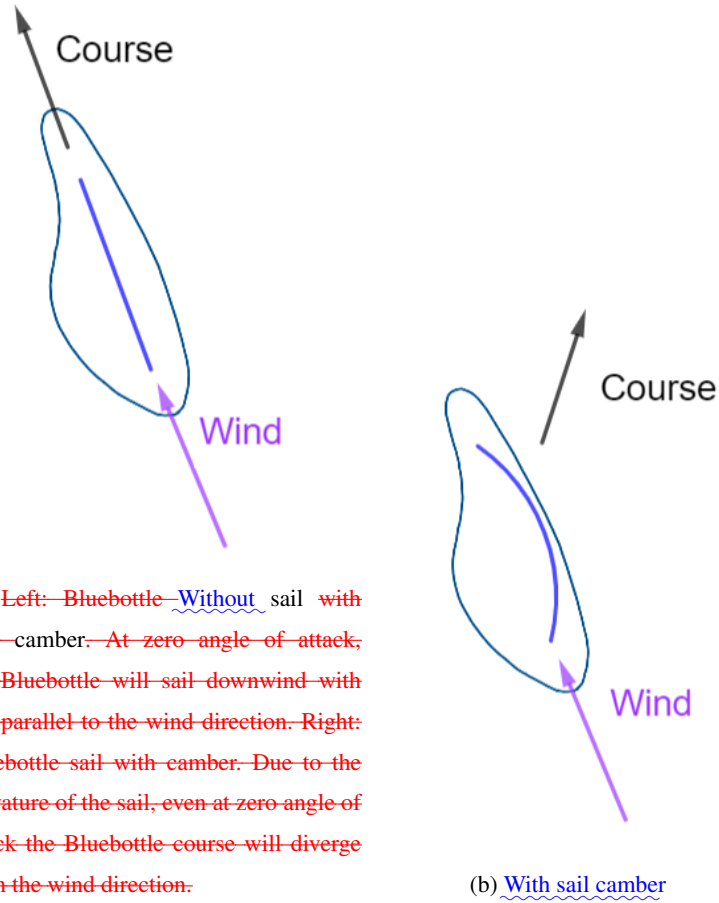


**Figure 6.** Bluebottle course at zero angle of attack is dependent on the sail camber. Panel (a) shows a Bluebottle with no camber sailing straight downwind with sail parallel to the wind direction. Panel (b) shows a Bluebottle with camber. Due to the curvature of the sail, even at zero angle of attack the Bluebottle course will diverge from the wind direction.

and  $\mathbf{R}$  is the identity matrix. Using Equation 16 Eq. (16) also gives this result. This gives a form that we have seen in previous literature (discussed in Sect. 6):

$$\mathbf{V}_{bb} = \mathbf{u} + \lambda \mathbf{V}_A. \quad (19)$$

We can also exclude the current by assuming  $\mathbf{u} = \mathbf{0}$  to reach another form seen in previous literature:

$$\mathbf{V}_{bb} = \lambda \mathbf{V}_A. \quad (20)$$

Hence we see that the models used in previous literature can be verified by our generalised form, but require fairly strong assumptions of downwind course zero angle of attack in all conditions and no camber. In Sect. 5.2 and 5.3 we lift these assumptions to further explore the drifting dynamics of the Bluebottle.

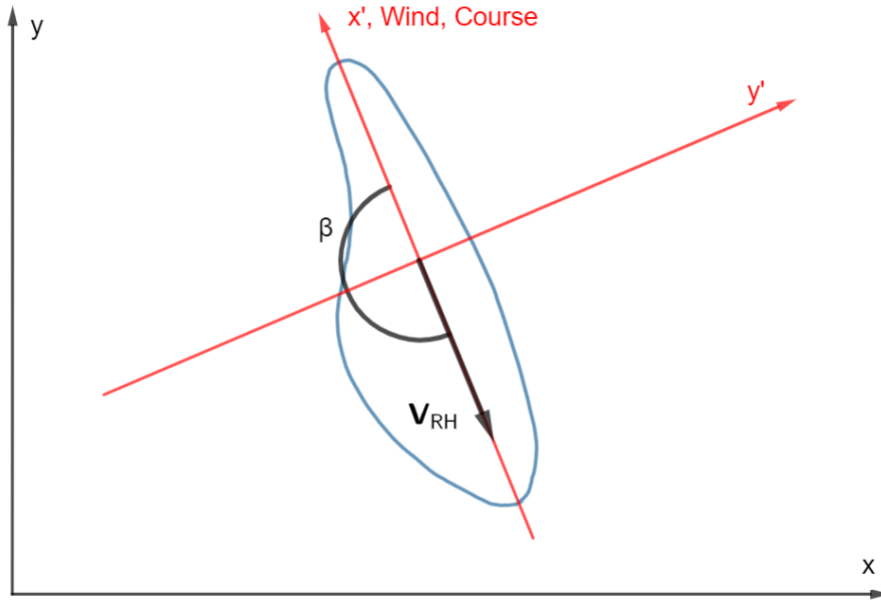


**Figure 7.** Case with no current and for a left-handed (right-sailing) Bluebottle sailing straight downwind with sail parallel to the wind direction ( $\beta_a = 0$ ). Note that the wind direction and BB-Bluebottle course are on the  $x'$  axis. A right-handed (left-sailing) Bluebottle would have the exact same course in this case.

It should be noted that, according to our model, a course straight downwind can also occur if the Bluebottle has an angle of attack of  $90^\circ$  (Fig. 5 and Fig. ??). However, Totton and Mackie (1960) did not observe angles of attack greater than  $40^\circ$  to  $45^\circ$  in their physical experiments. Hence we assume that the Bluebottle cannot orient at an angle of attack of  $90^\circ$ .

## 295 5.2 Case with angle of attack of $40^\circ$ and no current

Totton and Mackie (1960) observed that in light winds the PMW balances itself at approximately  $40^\circ$  to  $40^\circ$  to the wind. Hence, we now assume  $\beta_a$  has a value of  $40^\circ$  or  $-40^\circ$ , depending on whether the Bluebottle is right-handed (left-sailing) or left-handed (right-sailing), respectively. Since the orientation of the Bluebottle is constant relative to the wind, the sail is always hit by the wind at the same angle and the force coefficients  $C_{Ax'}$  and  $C_{Ay'}$  can be considered as constants. For  $C_{Ax'}$  we will use the value 0.1 as explained in Sect. 4.2. For  $C_{Ay'}$  we use the equation in Sect. ?? Eq. (18), giving a value of 0.40. We assume a camber ratio of 1%, the same as the value used in Iosilevskii and Weihs (2009). Recall that  $C_{Ay'}$  varies depending on the angle of attack. For example, from 0.31 to 0.50 for an angle of attack of  $30^\circ$  to  $50^\circ$ .

Assuming there is no current, our form simplifies to (Eq. (15)) simplifies to

$$\mathbf{V}_{bb} = \lambda \mathbf{R}(180^\circ - \beta + \beta_a) \mathbf{V}_A.$$

305  $\beta$  can be calculated using equation 8 Eq. (8) to be  $87.1^\circ$  (varies from  $86.2^\circ$  to  $87.7^\circ$  for an angle of attack of  $30^\circ$  to  $50^\circ$ ), while  $\lambda$  is calculated using equation 9 Eq. (9) to be 0.0266 (varies from 0.023 to 0.030 for an angle of attack of  $30^\circ$  to  $50^\circ$ ). We will

consider an example with a left-handed (right-sailing) Bluebottle, thus  $\beta_a = -40^\circ$ . Substituting all these values gives

$$\mathbf{V}_{bb} = 0.0266\mathbf{R}(52.9^\circ)\mathbf{V}_A.$$

We now have a clockwise rotation matrix. Hence, this means that the left-handed Bluebottle will drift at an angle of  $52.9^\circ$  clockwise (to the right) from the wind at 2.66% of the wind speed. Similarly, a right-handed Bluebottle will drift at an angle of  $52.9^\circ$  anticlockwise (to the left) from the wind at 2.66% of the wind speed. Note that since there is no current, the hydrodynamic force is only the drag from the submerged part of the Bluebottle. Hence the relative current vector  $\mathbf{V}_{RH}$  is directly opposite the Bluebottle's motion (Fig. 8).

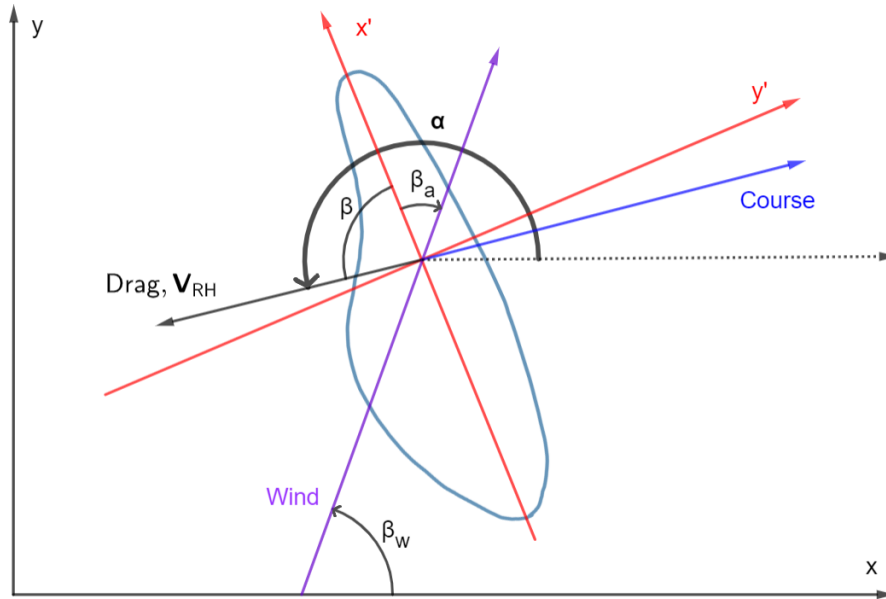


**Figure 8.** Case with no current for a left-handed (right-sailing) Bluebottle ( $\beta_a = -40^\circ$ ). Note that  $\beta_a$  is negative because it is the angle between the  $x'$  axis and the wind, which is clockwise. Length of Course and  $\mathbf{V}_{RH}$  are to scale. Wind vector length has been scaled down by a factor of 8.

### 5.3 Case with angle of attack of $40^\circ$ with current

315 Including the current does not have any impact on the calculated values of  $\beta$  or  $\lambda$ . Hence, the effect of the wind on the Bluebottle's speed and orientation will remain the same. By adding the current we have:

$$\mathbf{V}_{bb} = \mathbf{u} + 0.0266\mathbf{R}(52.9^\circ)\mathbf{V}_A.$$

Unlike Sect. 5.2, ~~with the ocean current added~~ considering the effect of background ocean current means that the relative current velocity  $\mathbf{V}_{RH}$  is no longer directly opposite the Bluebottle's course (Fig. 9). However, since the wind conditions and



320 other variables have not changed from Sect. 5.2, the aerodynamic force is identical. Hence, we also require the relative current vector to be identical since this determines the hydrodynamic force, which must balance out the aerodynamic force in order to have an equilibrium condition. This means that the course of the Bluebottle must adjust such that  $\mathbf{V}_{RH}$  is in the same position as Sect. 5.2 ( $\beta = 87.1^\circ$ ). ~~Fig.~~ Figure 10 shows examples of different current conditions with a constant wind. In each example,  $\mathbf{V}_{RH}$  is kept in the same position by adjusting the Bluebottle's course.

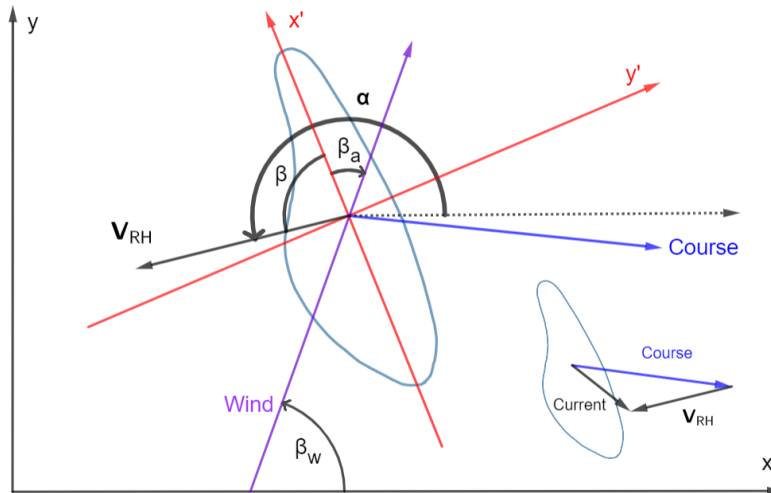


**Figure 9.** Case with current running south-east for a left-handed (right-sailing) Bluebottle ( $\beta_a = -40^\circ$ ). Diagram in the bottom right shows the vector addition between the Bluebottle's course, the current and the relative current felt by the Bluebottle. Length of Course, Current and  $V_{RH}$  are to scale, based on a current speed that is 5% of the wind speed. Wind vector length has been scaled down by a factor of 8.

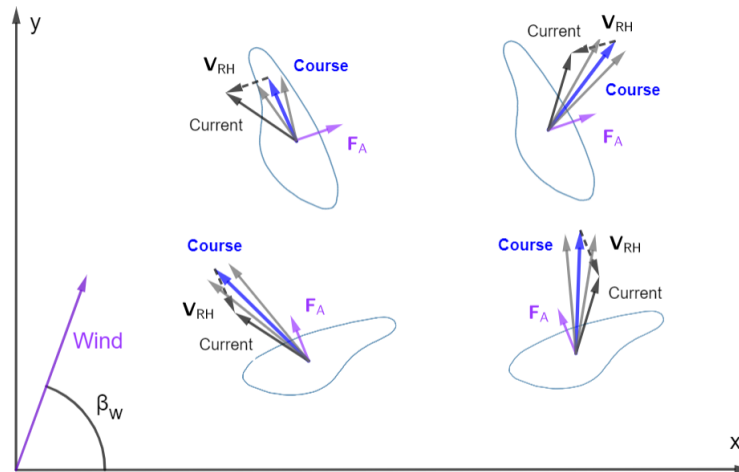


**Figure 10.** Examples of different currents with ocean current directions for a constant wind. Top row depicts left-handed (right-sailing) Bluebottles. Bottom row depicts right-handed (left-sailing) Bluebottles for the same wind and current conditions. Grey vectors indicate confidence intervals for the Bluebottle course if we consider that the angle of attack ( $\beta_a$ ) could be 30 to 50°. Note that for each form,  $V_{RH}$  must always point in the same direction. Length of Course, Current and  $V_{RH}$  are to scale, based on a current speed that is 5% of the wind speed. Wind vector length has been scaled down by a factor of 8.

## 325 6 Discussion and ~~Conclusion~~conclusion

We have added the ocean background current to an existing theoretical model ~~, taking the of~~ aerodynamic and hydrodynamic forces acting on ~~the Bluebottle and solving the a~~ Bluebottle. We then solve for an equilibrium condition to create a generalised vector model for the speed and course of the Bluebottle. Adding assumptions to our generalised model results in simplification to models that have been seen in previous literature. The generalised vector form is the link between the practical papers that  
330 used simple Lagrangian vector models and the theoretical papers that used a bottom-up approach. We also identify and discuss the key parameters: shape ( $\lambda$ ), angle of attack and camber. Finally, we find that under typical sailing conditions ~~the reported in~~ the literature (angle of attack of  $40^\circ$ ), the Bluebottle will drift at an angle of  $52.9^\circ$  from the wind at 2.66% of the wind speed, plus the velocity of the ocean background current.

It is worth noting that the form of equations 15 and 16 are different from leeway methods, which consider the motion of  
335 the object as a wind vector plus leeway (divergence from the wind). The leeway is often estimated using physical experiments and statistics. This methodology has been used in many previous studies (Breivik et al. (2011), Hackett et al. (2006), Ni et al. (2010), Wang et al. (2015)). Our theoretical bottom-up approach to calculate Bluebottle drift using force balance in equilibrium is a completely different methodology, despite the similar looking vector form that results from both techniques.

Our results compare well with previous Lagrangian model parametrizations. Ferrer and Pastor (2017) modelled the drift velocity of PMWs as wind velocity multiplied by a wind drag coefficient estimated from numerical simulations. The current was not used because wind was considered to be the main mechanism, based on Ferrer et al. (2014) who used symmetric fish tags for model calibration. The model calibration used in Ferrer et al. (2014) included a calculation of surface current as the combination of ROMS (Regional Ocean Modeling System) current and wind. They also ~~assume~~ assumed that the PMWs drift  
345 straight downwind. This matches our form in ~~equation 20~~ Eq. (20), where we assume the Bluebottle has zero angle of attack and there is no current. The model used by Prieto et al. (2015) was advection by surface currents (computed by ROMS model) plus 10% of wind velocity. This matches our form in ~~equation 19~~ Eq. (19), still assuming an angle of attack of zero. In comparison, we have a generalised form for calculating the drift of a Bluebottle for different angles of attack. We use a bottom-up approach for our wind velocity coefficient  $\lambda$ , which is determined by the specific areas and force coefficients of the ~~bluebottle~~ Bluebottle.  
350 We find that when the ~~bluebottle~~ Bluebottle has an angle of attack of  $40^\circ$ , as suggested by observations,  $\lambda = 0.0266$  and the wind pushes the ~~bluebottle~~ Bluebottle on a course of about  $53^\circ$  to the wind. This value of  $\lambda$  falls within the range of 0.02-0.045 tested by Ferrer and Pastor (2017) but differs from the 10% used by Prieto et al. (2015). The wind drift angle of  $53^\circ$  is similar to the  $45^\circ$  observed by Totton and Mackie (1960) and used amongst others in the model of Ferrer and González (2020). The  $\alpha$  term in our model accounts for the angle of the current, the angle of the wind and the ~~bluebottle~~ Bluebottle's angle of attack.  
355 Our model also incorporates the current, which has a significant effect even at ~~10m/s~~  $10 \text{ m s}^{-1}$  winds. Indeed, at wind speeds of  $O(10)$ , the speed imparted onto the Bluebottle from the wind is about  $0.266 \text{ m /ss}^{-1}$  (2.66% of wind speed), which is the same order of magnitude as the speed of ocean currents. Hence based on our vector form, the current should not be ignored when predicting the drift of the ~~bluebottle~~ Bluebottle. Note that the current relevant for this study is the surface ocean current which

would be felt by the ~~10cm~~ 10 cm Bluebottle. Relatively good results from modelling studies which did not take into account  
 360 the ocean current can be explained by the great impact the wind has on the top few centimeters of the ocean.

It should be noted that the influence of waves is not taken into account in our model. The impact forces of waves has an  
 effect on drifters (Szelangiewicz and Żelazny (2018)), but several additional variables and functions are required to calculate  
 this impact force. This will make our model significantly more complex, and currently cannot realistically be added. The effect  
 of Stokes drift, however, could be added into the ocean surface current vector, following Clarke and Vander (2018) for instance.  
 365 Stokes drift is a phenomenon that occurs on the ocean surface where the surface waves affect the net particle movement in  
 the top 1 or ~~2m~~ 2 m of the ocean, in the direction of the waves. Clarke and Vander (2018) found that Stokes drift is mostly  
 in the direction of the wind, and thus it is mainly due to shorter waves generated by the local wind. It was also found that the  
 magnitude of Stokes drift can be approximated by

$$u_{\text{Stokes}} = 4.4u_* \ln\left(\frac{0.0074u_{10}}{u_*}\right) \quad (21)$$

370 where  $u_{10}$  is the 10m wind speed and  $u_*$  is a parameter calculated by

$$u_* = \sqrt{\frac{|\tau_o|}{\rho_w}} \sqrt{\frac{|\tau_0|}{\rho_w}} \quad (22)$$

where  $|\tau_o|$  ~~is~~ is the wind stress magnitude and  $\rho_w$  is the density of water. Assuming a constant drag coefficient, Clarke and  
 Vander (2018) then show that  $u_{\text{Stokes}}$  can be estimated as 1% of  $u_{10}$ . This Stokes drift estimate can be added as an additional  
 term to ~~equation 15~~ Eq. (15), giving

$$375 \mathbf{V}_{\text{bb}} = \mathbf{u} + 0.01\mathbf{V}_A + \lambda\mathbf{R}(180^\circ - \beta + \beta_a)\mathbf{V}_A. \quad (23)$$

However, another consideration is that large waves (at high wind speeds) may break on top of the Bluebottle and result in  
 the Bluebottle becoming imbalanced or even toppling over. Our model cannot predict the behaviour of the Bluebottle in this  
 situation.

380 An assumption we used in Section 5 was a constant value for the angle of attack. In reality, the orientation of the Bluebottle  
 would be influenced by a combination of the wind and current conditions. In particular, observations suggest that the angle  
 of attack decreases from about 40° to 0° as wind speed increases (Totton and Mackie (1960)). More information from lab  
 experiments and in-situ surveys in the future are required to determine the value of this key parameter and its variability.  
 Instead of using a constant value for the angle of attack, it could be implemented in the model as a function of wind speed for  
 385 example.

Another assumption in ~~our~~ the model is that the body of the Bluebottle is assumed to be a perfectly symmetrical cylinder  
 with no tentacles. In reality, the submerged body is not perfectly symmetrical so the hydrodynamic force would also influence  
 the orientation of the Bluebottle's sail and body to some extent, like the keel of a sailboat. However, since the Bluebottle can  
 extend and retract the tentacle, changing its length and angle, it is hard to model. The drag force from the Bluebottle's single

390 tentacle (calculated using equations from Iosilevskii and Weihs (2009)) is  $O(10^{-2})$ , which is insignificant compared to the overall hydrodynamic force acting on the Bluebottle of  $O(1)$ .

This study is focused on the Bluebottles found on the east coast of Australia. Different parameter values may be required for the larger PMW. For example, Iosilevskii and Weihs (2009) use an estimate of 0.7 for the aspect ratio of the PMW's sail, 395 which affects the force coefficient  $C_{Ay'}$  (Sect. ~~??4.2~~). This is much larger than our measured aspect ratio for the Bluebottle's sail of 0.35. In Sect. 5.2 we conclude that at an angle of attack of  $40^\circ$  and no current, a left-handed Bluebottle will drift at an angle of  $52.9^\circ$  clockwise from the wind at 2.66% of the wind speed. A PMW in the same conditions will drift at an angle of  $51.5^\circ$  clockwise from the wind at 3.73% of the wind speed. While the drift angle is almost the same, the velocity of the PMW is 40% higher than the Bluebottle due to the higher aspect ratio leading to a larger force coefficient  $C_{Ay'}$ . It is worth noting 400 that the drag caused by the PMW's many long tentacles may affect its velocity significantly more than for the Bluebottle.

Further research that would supplement this study ~~and potentially lead to the prediction of Bluebottle beachings~~ include:

- physical experiments to observe Bluebottle drifting and estimate the key parameter values (e.g. force coefficients, angle of attack, camber) of our model.
- a detailed understanding of the specific habitat and life cycle of the Bluebottle to determine the starting point for a drift 405 model.

We hope our work, creating a generalised model for Bluebottle drift, encourages new research in this area and helps in the ~~future development of~~ development of accurate numerical tracking and, ultimately, a forecasting tool that can prevent tens of thousands of beachgoers from experiencing painful Bluebottle stings.

## 1 Appendix A

410 *Author contributions.* D.L. led the writing of the manuscript, completed the derivations and performed the calculations. A.S. contributed to writing the manuscript and the derivations. S.G. provided the idea and helped with derivation and writing of the manuscript.

*Competing interests.* The authors declare that they have no conflict of interest.

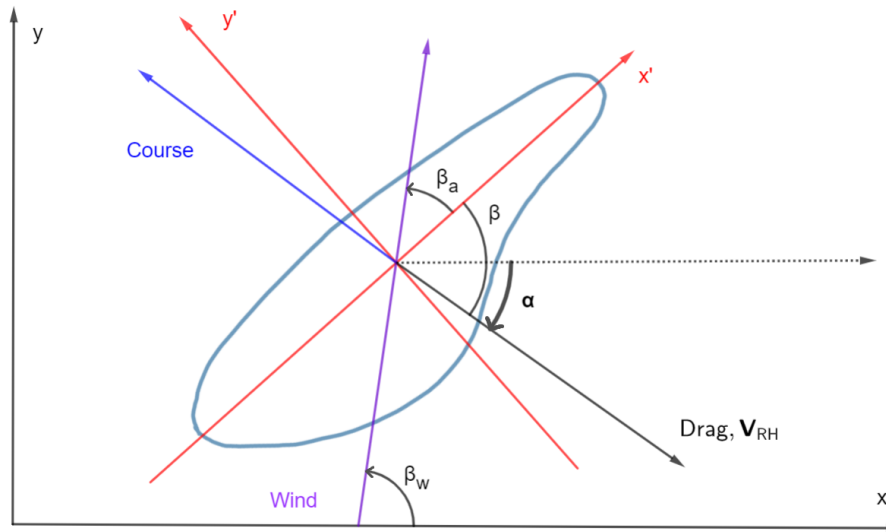


**Figure A1.** Case with no current for a right-handed (left-sailing) Bluebottle ( $\beta_a = 40^\circ$ ). Length of Course and  $V_{RH}$  are to scale. Wind vector length has been scaled down by a factor of 8.

## References

- Abbott, I., Doenhoff, A., and Stivers, L.: Summary of Airfoil Data, 1945.
- 415 Breivik, O., Allen, A., Maisondieu, C., and Roth, J.: Wind-induced drift of objects at sea: The leeway field method, *Applied Ocean Research* - APPL OCEAN RES, 33, <https://doi.org/10.1016/j.apor.2011.01.005>, 2011.
- Clarke, A. and Vander, S.: The Relationship of Near-Surface Flow, Stokes Drift and the Wind Stress, *Journal of Geophysical Research: Oceans*, 123, 2018.
- Ferrer, L. and González, M.: Relationship between dimorphism and drift in the Portuguese man-of-war, *Continental Shelf Research*, p. 420 104269, <https://doi.org/10.1016/j.csr.2020.104269>, 2020.
- Ferrer, L. and Pastor, A.: The Portuguese man-of-war: Gone with the wind, *Regional Studies in Marine Science*, 14, <https://doi.org/10.1016/j.rsma.2017.05.004>, 2017.
- Ferrer, L., Zaldua-Mendizabal, N., del Campo, A., Franco, J., Mader, J., Cotano, U., Fraile, I., Rubio, A., Uriarte, A., and Caballero, A.: Operational protocol for the sighting and tracking of Portuguese man-of-war in the southeastern Bay of Biscay: Observations and modeling, *Continental Shelf Research*, 95, <https://doi.org/10.1016/j.csr.2014.12.011>, 2014.
- 425 Hackett, B., Breivik, O., and Wettre, C.: Forecasting the Drift of Objects and Substances in the Ocean, pp. 507–523, Springer Netherlands, [https://doi.org/10.1007/1-4020-4028-8\\_23](https://doi.org/10.1007/1-4020-4028-8_23), 2006.
- Headlam, J. L., Lyons, K., Kenny, J., Lenihan, E. S., Quigley, D. T., Helps, W., Dugon, M. M., and Doyle, T. K.: Insights on the origin and drift trajectories of Portuguese man of war (*Physalia physalis*) over the Celtic Sea shelf area, *Estuarine, Coastal and Shelf Science*, 2020.
- 430 Iosilevskii, G. and Weihs, D.: Hydrodynamics of sailing of the Portuguese man-of-war *Physalia physalis*, *Journal of the Royal Society, Interface / the Royal Society*, 6, 613–26, <https://doi.org/10.1098/rsif.2008.0457>, 2009.

- Munro, C., Vue, Z., Behringer, R., and Dunn, C.: Morphology and development of the Portuguese man of war, *Physalia physalis*, *Scientific Reports*, <https://doi.org/10.1101/645465>, 2019.
- Ni, Z., Qiu, Z., and Su, T.: On predicting boat drift for search and rescue, *Ocean Engineering - OCEAN ENG*, 37, 1169–1179, <https://doi.org/10.1016/j.oceaneng.2010.05.009>, 2010.
- 435 Prieto, L., Macías, D., Peliz, A., and Ruiz, J.: Portuguese Man-of-War (*Physalia physalis*) in the Mediterranean: A permanent invasion or a casual appearance?, *Scientific Reports*, 5, <https://doi.org/10.1038/srep11545>, 2015.
- Shannon, P. and Chapman, L.: Incidence of *Physalia* on beaches in the south-western Cape Province during January 1983, *South African Journal of Science*, 79, 454, [https://doi.org/10.10520/AJA00382353\\_5954](https://doi.org/10.10520/AJA00382353_5954), 1983.
- 440 Surf Life Saving Australia: Sydney: National Coastal Safety Report 2020, 2020.
- Szelangiewicz, T. and Żelazny, K.: Mathematical Model for Predicting the Ship Speed in the Actual Weather Conditions on the Planned Ocean Route, *New Trends in Production Engineering*, 1, 105–112, <https://doi.org/10.2478/ntpe-2018-0013>, 2018.
- Totton, A. and Mackie, G.: Diphormism in the Portuguese-Man-of-War, *Nature*, 177, 290, 1956.
- Totton, A. and Mackie, G.: Studies on *Physalia physalis*, *Discovery Reports*, 30, 301–368, cited By 43, 1960.
- 445 Wang, S.-Z., Nie, H.-B., and Shi, C.-J.: A drifting trajectory prediction model based on object shape and stochastic motion features, *Journal of Hydrodynamics, Ser. B*, 26, [https://doi.org/10.1016/S1001-6058\(14\)60104-9](https://doi.org/10.1016/S1001-6058(14)60104-9), 2015.
- Woodcock, A. H.: A theory of surface water motion deduced from the wind-induced motion of the *Physalia*, *Journal of Marine Research*, 5, 196, 1944.